Optics & Laser Technology 44 (2012) 1689–1697

Contents lists available at SciVerse ScienceDirect

Optics & Laser Technology

journal homepage: www.elsevier.com/locate/optlastec

Structural, optical and electrical characteristics of a new NLO crystal

E.D. D'silva [a,*], G. Krishna Podagatlapalli [b], S. Venugopal Rao [b], S.M. Dharmaprakash [a]

[a] Department of Studies in Physics, Mangalore University, Mangalagangotri, Mangalore 574199, India
[b] Advanced Centre of Research in High Energy Materials (ACRHEM), University of Hyderabad, Hyderabad 500046, India

ARTICLE INFO

Article history:
Received 21 October 2011
Received in revised form
23 December 2011
Accepted 12 January 2012
Available online 4 February 2012

Keywords:
Nonlinear optical material
Third-harmonic generation
Laser damage threshold

ABSTRACT

A new nonlinear optical (NLO) organic crystal 1-[4-({(*E*)-[4-(methylsulfanyl)phenyl]methylidene}amino)phenyl]ethanone (MMP) has been grown by slow evaporation technique at ambient temperature. The crystal structure of MMP was determined by single crystal X-ray diffraction. MMP crystallizes in non-centrosymmetric monoclinic system with space group $P2_1$. The FT-IR spectrum recorded for new crystal confirmed the presence of various functional groups in the material. MMP was found to be thermally stable up to 300 °C. The grown crystal was optically transparent in the wavelength range of 400–1100 nm. The second harmonic generation (SHG) efficiency of the crystal was measured by the classical powder technique using Nd:YAG laser and was found to be 4.13 times more efficient than reference material, urea. Third order nonlinear parameters were measured by employing the Z-scan technique. The laser damage threshold for MMP crystal was determined to be 4.26 GW/cm^2. The Brewster angle technique was employed to measure the refractive index of the crystal and the values for green and red wavelengths were found to be 1.35 and 1.33, respectively. The dielectric and electrical measurements were carried out to study the different polarization mechanisms and conductivity of the crystal.

1. Introduction

The development of optical devices, such as photonic integrated circuitry, depends strongly on the design of highly efficient nonlinear optical (NLO) materials. Among such NLO materials, organic materials are shown to be superior to their inorganic counterparts in terms of synthesis, crystal fabrication, potential to create large devices and much faster optical nonlinearities [1,2]. Various organic single crystals like stilbazolium crystals [2], OH1 [3] and crystals of other charge transfer complexes [4], such as chalcones [5], have been attractive for frequency conversion, integrated circuitry and terahertz (THz) applications [6]. Organic derivatives having polarizable electrons (e.g., π-electrons) spread over a large distance with various combinations of terminal electron donor and/or acceptor groups have been the objective of recent research, particularly in view of their large molecular hyperpolarizabilities and good crystallizability [7–11], which may lead to a wide range of applications in integrated optics (second harmonic generation (SHG), frequency mixing, electro-optic modulation, parametric effects, etc.) [12,13]. The design and synthesis of organic molecules exhibiting second-order nonlinear optical (NLO) properties has also been motivated by their tremendous potential for application in optical communications, optical computing, data storage, dynamic holography, harmonic generators, frequency mixing and optical switching [10,14]. In this perspective the synthesis, growth and various characterization studies of crystal (MMP), possessing π-conjugated donor–π–acceptor system is imperative to explore its possible applications in nonlinear optics. The nonlinearity in the organic materials originates from a strong delocalization of 'π' electrons along the length of molecules [15]. It is, therefore, possible to tune or tailor the molecular structure to enhance the nonlinear optical properties. Most of the optical device applications also require a thorough understanding of its third order nonlinear optical properties, which is an important part of this investigation. Second harmonic generation (SHG) efficiency of crystalline materials depends both on the magnitude of molecular hyperpolarizability (β) and on the orientation of the molecules in the crystal lattice [16]. Organic molecules, in general, are potentially more attractive and versatile than inorganic compounds because of their large β-values, fast response time, high resistance to optical damage and almost unlimited possibilities of designing molecules suitable for SHG [17,18]. But practical applications are limited due to poor chemical stability, absorption of visible light due to conjugation, poor phase matching properties and inability to grow bulk crystals. This paper deals with the details of synthesis, growth, structure and characterization of a new organic material MMP.

* Corresponding author. Tel.: +91 8970093263; fax: +91 8242287367.
E-mail address: deepak.dsilva@gmail.com (E.D. D'silva).

0030-3992/$ - see front matter © 2012 Elsevier Ltd. All rights reserved.
doi:10.1016/j.optlastec.2012.01.017

The molecular structure of present crystal consists of *N*-[(*E*)-phenylmethylidene]aniline unit, attached with two groups $COCH_3$ (electron acceptor) and SCH_3 (electron donor) to form 1-[4-({(*E*)-[4-(methylsulfanyl)phenyl]methylidene}amino)phenyl]ethanone (MMP). The methylidene backbone is an asymmetric transmitter and increases molecular nonlinearity for electron donating and withdrawing group substitutions.

2. Experimental procedure

Commercially available 4-aminoacetophenone and 4-methylthiobenzaldehyde were used without further purification. A mixture of equimolar quantities (0.01 M each) of 4-aminoacetophenone (Sigma-Aldrich 99% pure) and 4-methylthiobenzaldehyde (Sigma-Aldrich 95% pure) in ethanol (60 ml) were stirred for 2 h. Then the contents of flask were poured into ice cold water (250 ml) and left for 12 h. The resulting crude solid was collected by filtration, dried and purified by repeated crystallization from acetone. The schematic representation of the reaction is given in Scheme 1. The solubility of the compound was determined by adding solvent to a known amount of compound till it was completely dissolved. It was found that compound was insoluble in water, soluble in acetone, methanol and N, N-dimethyl formamide (DMF). Methanol was found to be the best solvent for MMP crystal. Single crystals of MMP were grown in methanol solution using the slow evaporation technique at ambient temperature. Crystals grown in solvent acetone were not transparent, due to high rate of evaporation.

The single crystal X-ray diffraction data was collected on Bruker Kappa Apex using Apex2 software package. The radiation used was graphite monochromatic MoK_α radiation. All the data were corrected for Lorentz factor and empirical absorption. The structure was solved by direct method and all the non-hydrogen atoms and hydrogen atoms were found in difference electron density maps. The atomic coordinates and anisotropic temperature factors for non-hydrogen atoms were refined by the full-matrix least square method using SHELXTL program package [19]. The FT-IR analysis of MMP was carried out to investigate the presence of functional groups and their vibrational modes [20]. The sample was prepared by mixing MMP with KBr pellet. The spectrum was recorded between 400 and 4000 cm^{-1} using a Thermo Nicolet Avatar, 370 FT-IR spectrometer. To investigate the thermal stability [21] of MMP, thermogravimetric analysis was carried out. Powdered sample of the crystal was selected for this purpose and the analysis was carried out under the nitrogen atmosphere at a heating rate of 10 °C/min using Perkin-Elemer simultaneous TGA/DTA analyzer. The UV–VIS–NIR absorption spectrum of the crystals was recorded using a Cary 5E high resolution spectrophotometer, in the wavelength range of 350–1100 nm. Crystals with parallel surfaces and thickness of ~1 mm were used for this purpose.

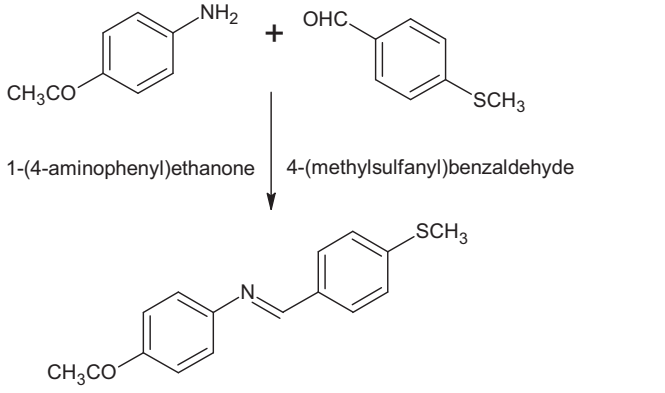

1-[4-({(*E*)-[4-(methylsulfanyl)phenyl]methylidene}amino)phenyl]ethanone

Scheme 1. Synthesis of MMP.

In order to determine SHG efficiency, the crystal was ground into uniform powder and then packed in a micro-capillary of uniform bore and exposed to a Q-switched Nd:YAG laser of wavelength 1064 nm. The laser was incident normally on the sample capillary tube and output from the sample was passed through Monochromater to collect the intensity of 532 nm component. The Z-scan experiment was performed with a picosecond (ps) amplifier (seed pulse was from Micra laser oscillator (COHERENT)) generating ~2 ps pulses at a repetition of 1 kHz. The experiment was done at a wavelength of 800 nm. The average and peak powers were ~2 W, ~1 GW, respectively. The diameter of the beam from the amplifier was ~4 mm. Using ND filters the input energy/power was controlled. The laser damage threshold (LDT) studies were carried out on solution grown MMP single crystals using a Q-switched Nd:YAG laser source of pulse width 6 ns at a wavelength of 1064 nm and a 10 Hz repetition rate, operating in TEM_{00} mode. The refractive index value of the MMP crystal understudy was determined by employing the Brewster angle method. The linearly polarized light from the laser source operating in TEM_{00} mode was incident on plane surface of the crystal. He–Ne lasers of wavelength 543.5 (green) and 632.8 (red) are used as laser sources for the experiment. The dielectric properties were measured on the pellet samples using a Agilant 4263B LCZ metre for frequencies 100 HZ, 1k Hz, 10k Hz, 100k Hz with a applied voltage of 1 Vpp and over a temperature range of 30–110 °C. The sample was silver electrode by applying a thin layer of silver paint on both faces of the pellet. Then it was placed in a dry atmosphere for 24 h to ensure the maximum conductivity and adhesion of the silver paste. The pellet sample was mounted between two stainless steel electrodes being held by spring loaded contacts to form a cell consisting of parallel plate capacitor. For studying the effect of temperature on dielectric constant, the sample was enclosed in a resistance heated furnace and the temperature was monitored using a chromel–alumel thermocouple. The temperature of the sample was increased by regulating the input power. At each temperature the sample was kept for 15 min to ensure thermal equilibrium. The *I–V* dependence of the grown crystals were conducted using Kiethley 2361-V programmable source measured unit with METRICES-ICS software, by two probe method at room temperature. Crystal's pellets were pasted with good quality silver paint on both sides to ensure the good electrical contact. The measurements have been carried out in resistance mode by applying voltage in the range of 0–100 V, in steps of 2 V and current is measured.

3. Results and discussion

3.1. Crystal growth

Transparent plate like crystals appeared in the growth vessels within 2 weeks of solution evaporation. However bulk crystal with definite morphology of MMP did not grow, even after repeating the growth experiment several times. Only by continuous and repeated re-crystallization process it was possible to obtain good quality crystals. The crystals reached a maximum size of $4 \times 4 \times 2$ mm^3 over a time period of one month. Crystals obtained were non-hygroscopic and stable at room temperature. These crystals were white-reddish in color and grown in the form of plates (Fig. 1)

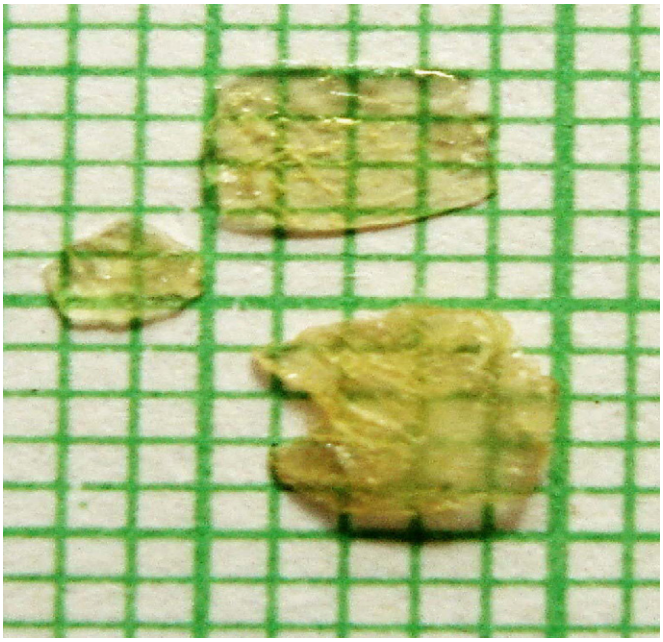

Fig. 1. Photograph of the crystal MMP.

Table 1
Crystal data and structure refinement.

Empirical formula	C16 H15 N O S
Formula weight	269.35
Temperature	223(2) K
Wavelength	0.71073 Å
Crystal system	Monoclinic
Space group	P2(1)
Unit cell dimensions	a=5.6741(5) Å, α=90°
	b=33.365(3) Å, β=90.136(2)°
	c=7.2064(6) Å, γ=90°
Volume	1364.30(19) Å^3
Z	4
Density (calculated)	1.311 Mg/m^3
Absorption coefficient	0.228 mm^{-1}
F(000)	568
Crystal size	0.24 × 0.16 × 0.10 mm^3
Index ranges	$-7<=h<=7$, $-43<=k<=36$, $-9<=l<=9$
Reflections collected	9548
Independent reflections	4903 [R(int)=0.0501]
Refinement method	Full-matrix least-squares on F^2

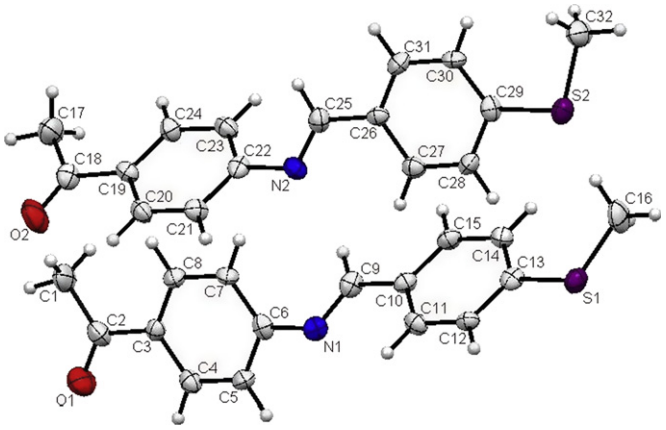

Fig. 2. Molecular structure of 4Br4MSP, drawn with 50% probability displacement ellipsoids and showing the atom labeling scheme.

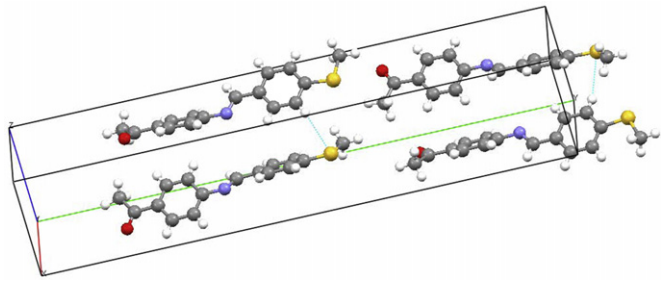

Fig. 3. Crystal packing when viewed down the c-axis.

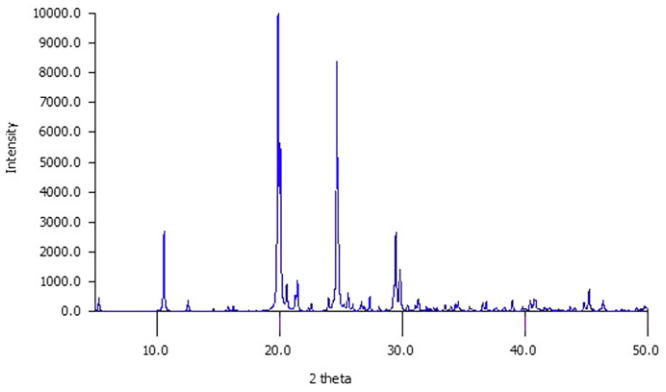

Fig. 4. X-ray diffraction pattern of MMP.

3.2. Crystal structure

From single-crystal XRD studies, it has been found that the compound crystallizes in the monoclinic system with a space group $P2_1$, which is considered as noncentrosymmetric system and thus satisfies the requirements for the SHG activity in the crystal. The crystal data is summarized in Table 1. Fig. 2 represents the ORTEP of molecule with thermal ellipsoids at 50% probability [22]. The crystal packing of MMP is shown in Fig. 3. The asymmetric unit contains two molecules of the compound $C_{16}H_{15}NOS$. These two molecules face the same direction and form a stack of molecules along the c-axis in the crystal packing. The crystal packing consisted of molecules which were arranged along b-axis perpendicular to plane ac. Along the row adjacent molecules were inverted and connected by head to tail fashion by the intermolecular O…H bonding. All bond distances and bond angles lied within the normal ranges. The crystal structure was stabilized by intermolecular (N–H, O–H, S–H) hydrogen bonds. The dihedral angles between the two aromatic rings within the two molecules were 52.44° and 52.09°. This indicates that aromatic rings are out of plane. The diffraction pattern has been indexed by least-square fit method. Fig. 4 shows the XRD patterns of the crystal generated from single crystal data using *mercury* software. The sharpness of the peak shows good degree of crystallinity. The planes corresponding to intensity peaks at 2θ angle 10.5°, 20°, 24.6°, 30° are indexed as (040), (101), (002), (062) respectively. X-ray diffraction pattern has highest intensity corresponding to (040) plane. The FT-IR spectrum is shown in Fig. 5. The characteristic transmission peaks are consistent with the functional groups present in the compound and the assigned values are as recorded in Table 2.

3.3. Optical properties

The UV–Vis–NIR spectrum of the crystal is depicted in Fig. 6. Most of the organic crystals including chalcone show wider

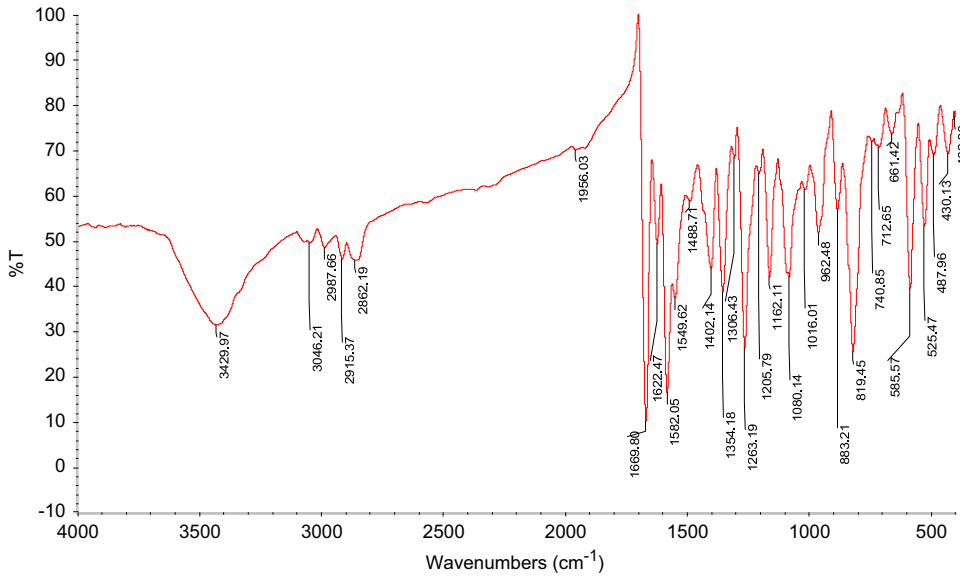

Fig. 5. FT-IR spectra of MMP.

Table 2
Functional group assignment of MMP from FT-IR spectrum.

Wave number (cm^{-1})	Mode assignment
3046.21	Aromatic-H stretch
2915.37, 2862.19	=C–H stretch, C–H stretch
1669.80	C=N
1582.05	C=C stretch (Ar. rings)
1549.62	Aromatic ring vibrations
1435.50	C–H deformation
1402.14	$COCH_3$
1162.11	C–N stretch (amine)
1080.14 and less	C–H aromatic bend (Ar–H)

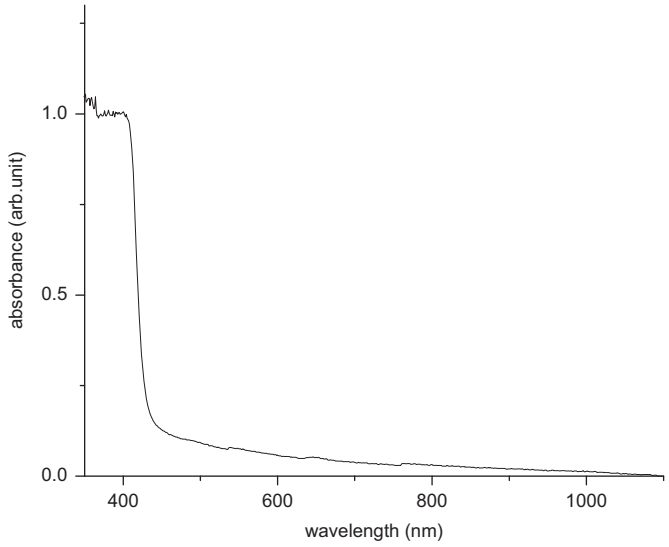

Fig. 6. UV–vis–NIR absorption spectrum of the MMP crystal.

transparency range extending into the entire visible and IR region. The cutoff wavelength for this crystal was found to be 400 nm. Above this range no absorption peaks were present until the IR spectral region. The maximum absorption was assigned for the $n \rightarrow \pi^*$ transition and may be attributed to the excitation of N=C group [23]. The wide transparency range will be helpful for these crystals to be used for NLO applications. In a crystalline material the region of transparency to the electromagnetic radiation defines the intrinsic loss mechanisms and also theoretical transmittance achievable within this region. The transparent spectral region in insulators at short wavelengths is defined by electronic transition across the band gap and at long wavelengths by lattice vibrations. The absorption coefficient consists of contribution from direct/indirect band gap transition, back ground absorption and scattering. The band gap of the material sets the limiting cut-off wavelengths λ_c defined by $\lambda_c = hc/Eg$. The optical band gap E_g is (Tauc's expression) [24] given by $\omega^2\varepsilon_2 = (h\omega - E_g)^2$. Where $\varepsilon_2(\lambda)$ is the imaginary part of the complex refractive index, that represents optical absorbance and E_g is usually obtained from the plot $\varepsilon_2^{1/2}/\lambda$ vs. $(1/\lambda)$. The intersection of the extrapolated spectrum with abscissa gives the gap wavelength λ_g, from which the gap energy is derived to be $E_g = hc/\lambda_g$.

The dependence of absorption coefficient α in terms of direct and indirect transitions is most often performed with the help of formula derived for the three-dimensional (3D) crystals. Their simplest form is as follows:

$$\alpha h\nu = A(h\nu - E_g)^r, \text{ for direct band gap}$$
$$\alpha h\nu = \sum_j A(h\nu - E_g \pm E_{pj})^r, \text{ for indirect band gap}$$

where α is the absorption coefficient, calculated as a function of photon energy. E_g is the energy gap for direct transition, E_g' is the energy gap for indirect transition and E_{pj} is the energy of the phonons assisting the direct transition. A and B are parameters depending more in complicated ways on temperature, photon energy, phonon energy E_p. Specifically the power $r=2$ is for indirect and $r=1/2$ for direct allowed transitions. The direct band gap can be obtained by plotting $(\alpha h\gamma)^{1/2}$ versus energy (eV). Indirect band gap can be obtained by plotting $(\alpha h\gamma)^2$ versus energy (eV).

The band gap values determined from $\varepsilon_2^{1/2}/\lambda$ versus $(1/\lambda)$, direct and indirect band gap (plotted in Fig. 7) methods were found to be 2.27 eV, 2.8 eV and 2.94 eV. The energy band gap values obtained by employing three different methods were comparable with each other. The high energy gap values confirmed that at room temperature MMP crystals were insulators.

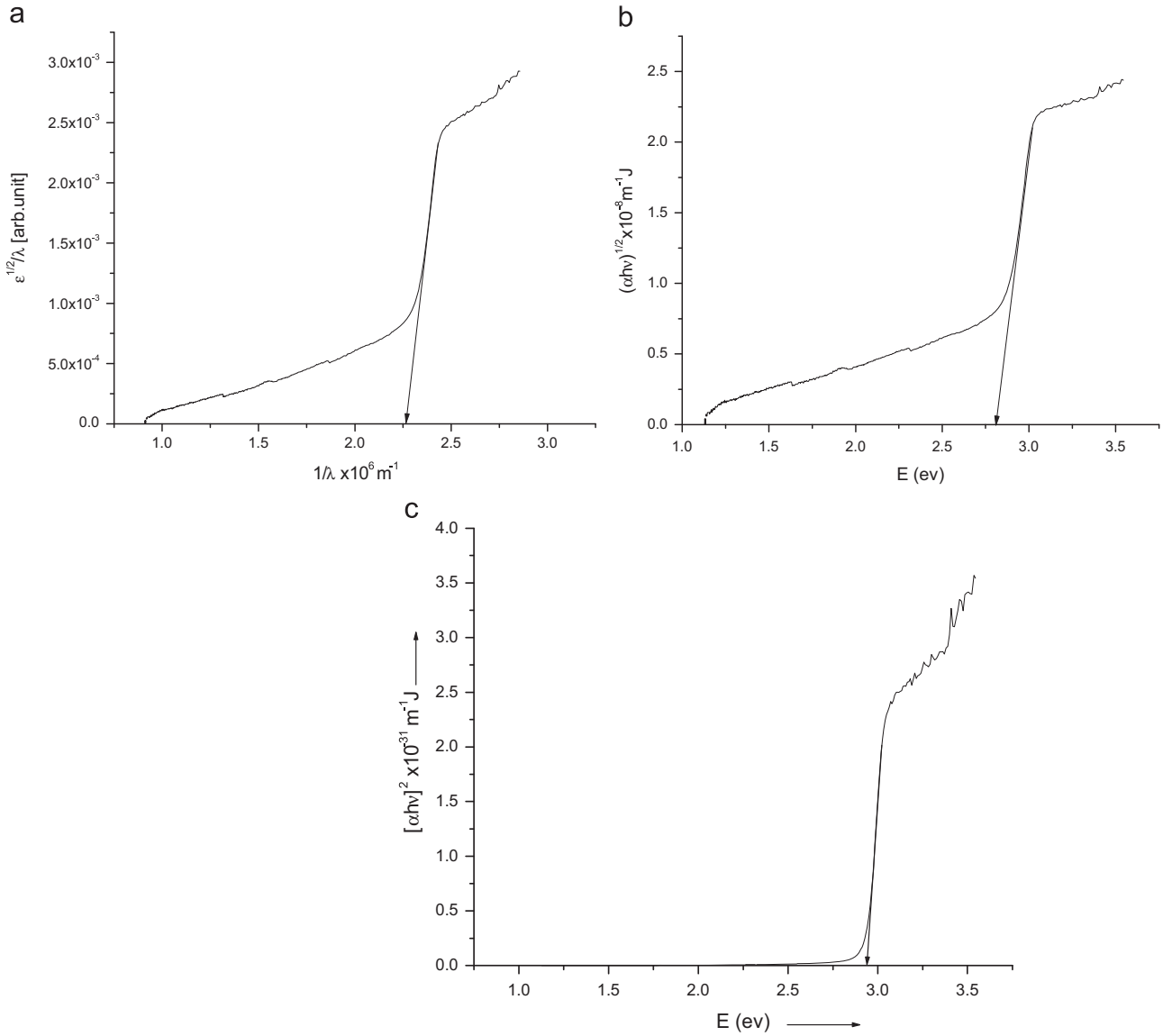

Fig. 7. Plot of (a)$\varepsilon_2^{1/2}/\lambda$ vs. $(1/\lambda)$, (b)$(\alpha h\gamma)^{1/2}$vs. E and (c) $(\alpha h\gamma)^2$ vs. E.

3.4. Thermal studies

The results of TG/DTA analysis are shown in Fig. 8. The DTA curve implies that the material undergoes an irreversible endothermic transition at 150 °C, where melting begins. The peak of the endothermic represents temperature 152.54 °C at which melting terminates, corresponding to the melting point of MMP crystal. It is clear from the DTA curve that there is no phase transition before melting. The sharpness of the peak demonstrated good crystallinity and purity of the sample. The TG curve of this sample indicates that the sample was stable up to 300 °C. The exothermic peak of the DTA at 363.6 °C, corresponding to the weight loss in the TG curve, indicated that the weight loss was due the degradation and evaporation of the sample. Melting point of MMP was determined by the open capillary method and was uncorrected. It has a quite high melting point of 152.5 °C, which was the same as measured by thermal analysis.

3.5. Laser light interaction

The method developed by Kurtz and Perry [25] is a simple setup to evaluate second harmonic generation (SHG) conversion efficiency of any nonlinear optical material, taken in its powder form. Here, the conversion efficiency of a given material is compared with standard reference materials like urea or potassium dihydrogen phosphate. A Q-switched Nd:YAG laser beam (of wavelength 1064 nm with an input power of 8 mJ, and a pulse width of 8 ns with a repetition rate of 10 Hz) was incident normally on the sample capillary tube and the output from the sample (S) was passed through a monochromater to collect the intensity of 532 nm component. The generation of second harmonic was confirmed by the emission of green light. The fundamental wave was eliminated by passing the beam through filter consisting of $CuSO_4$ solution, which absorbed the 1064 nm light. Another filter BG-38 also removed any residual 1064 nm light. Second harmonic radiation generated by the randomly oriented micro-crystals (of particle size less than 63 μm) was focused by a lens. The amplitude of the SHG output voltage was measured using photomultiplier and digitalizing oscilloscope assembly. The second harmonic (SH) signal was converted into electrical signal using a photomultiplier tube and was finally displayed on a digital storage oscilloscope. Similar procedure was employed to measure the amplitude of reference material urea, which was powdered to the identical particle size and taken in a capillary

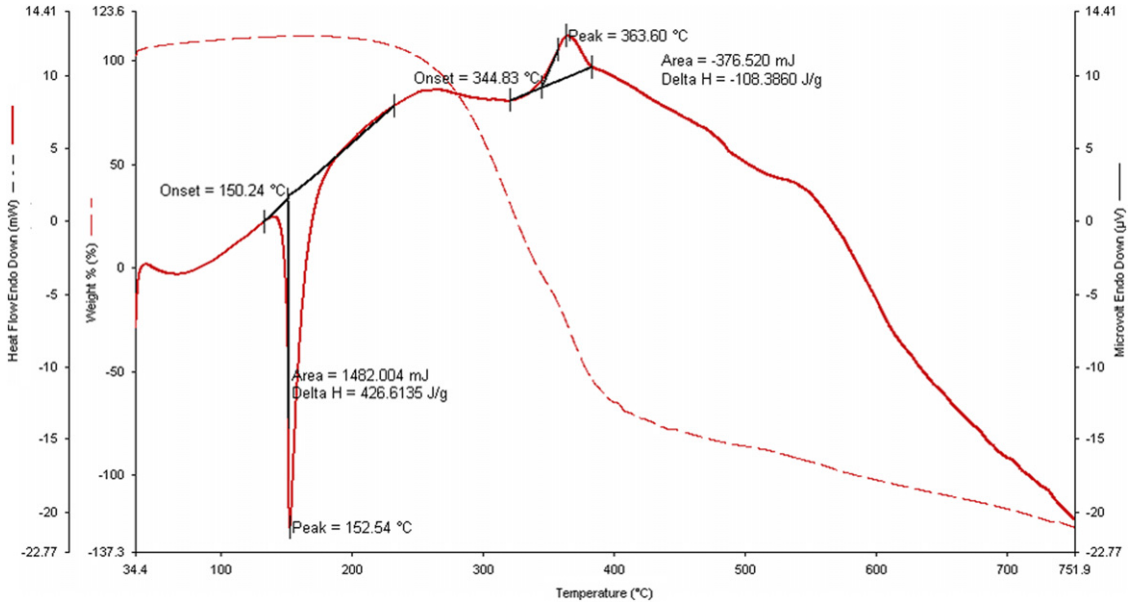

Fig. 8. TGA/DTA curve of the sample.

tube. The beam energy of the Nd:YAG laser was set to 3.2 mJ/pulse. The ratio of the amplitudes of the SHG signal was calculated. The second harmonic generation efficiency for MMP was found to be 4.13 times that of urea crystals of identical particle size. The MMP crystal can be considered as acceptor–π–donor system, where charge transfer takes place from donor (SCH3) to acceptor (COCH3) group through methylidene backbone. The presence of donor–acceptor groups, charge transfer axis, parallel head to tail arrangement in crystal packing, the number of intermolecular bonding enabled MMP to have higher SHG efficiency than urea.

To study the third-order NLO properties a single beam Z-scan technique was employed, which readily provides the magnitude and sign of nonlinearity. The laser beam was focused into 1 mm quartz cuvette that contained sample solution (dissolved in DMF solvent with 10^{-2} mol concentration) by using a 20 cm biconvex lens. The resulting beam waist radius at the focus was $\sim$25.44 µm, corresponding to a Rayleigh length of 2.54 mm. For measuring the refractive nonlinear property, an aperture was placed in front of the detector and the transmittance was recorded as a function of the sample position on the Z-axis (closed aperture Z-scan). For measuring the nonlinear absorption the sample transmittance was measured without the aperture as a function of sample position (open aperture Z-scan).

For a temporal Gaussian pulse with an incident Gaussian spatial profile, the on-axis transmission has been shown as a function of sample position relative to the lens focal point and the normalized transmittance for the open aperture Z-scan is given by [26]

$$T(Z) = 1 - \frac{\beta I_0 L_{eff}}{2\sqrt{2}} \frac{1}{(1+z^2/z_0^2)} \quad (1)$$

where I_0 is the peak irradiance at the focus, β is the nonlinear absorption coefficient, z_0 is the Rayleigh length given by the formula $z_0 = k\omega_0^2/2$ with k being the wave vector and ω_0 the beam waist radius at the focus and L_{eff} is the effective sample length. The open aperture Z-scan data (at 1 mW input power) of the sample is shown in Fig. 9. The nonlinear refraction data obtained by dividing the closed aperture Z-scan data by the open aperture data is presented in Fig. 10. The nonlinear absorption coefficient was determined by fitting the experimental open aperture Z-scan data with (1). Similarly, the nonlinear refractive index was obtained by fitting the closed aperture Z-scan experimental data with the equation given in

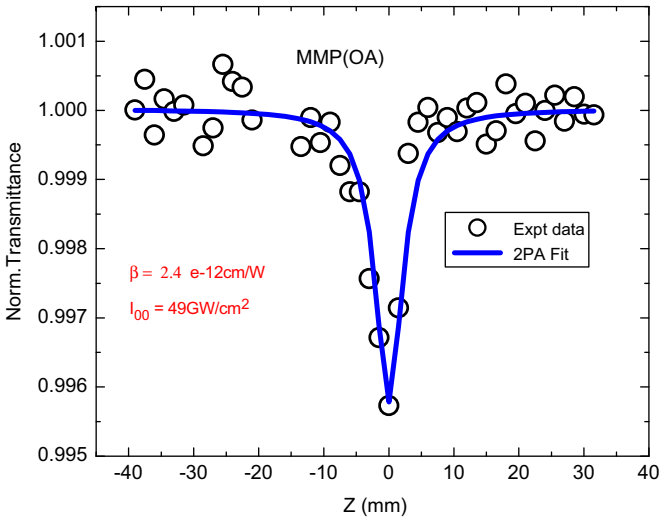

Fig. 9. Open aperture Z-scan curve of the MMP sample. The solid line is a theoretical fit of the experimental data.

[27]. The n_2, β_{eff}, Im$\chi^{(3)}$ and Re$\chi^{(3)}$ at 1 mW were found to be 9.67×10^{-14} esu, 2.4×10^{-12} cmW^{-1}, 0.15×10^{-22} m^2/V^2 and 2.9×10^{-22} m^2/V^2, respectively. The molecular hyperpolarizability of this chalcone calculated using the formula $\gamma_h = \chi(3)R/L^4N$, where L is the local field factor and N is the number of molecules per cubic centimeter, was 0.09×10^{-32} esu. The observed value of molecular hyperpolarizability is comparable with reported literature values for chalcones [28]. It was observed that β_{eff} increased with increase in I_0 and the intercept on the vertical axis was non-zero suggesting that a higher order effect, such as excited state absorption (ESA) via two photon absorption contributing to nonlinear absorption (NLA) was present. Attempts of understanding of third order NLO properties of organic crystals are very limited [29–32] and the third order nonlinear optical property is not imposed with any crystal symmetry restrictions. Various design strategies have been proposed for synthesizing molecules with large 2PAcross-sections. For example, Alabota et al. [31] proposed the synthesis of symmetric conjugated molecules with D–π–A–π–D, A–π–D–π–A or D–π–A structure and elongation of the conjugation length, whereas Reinhardt et al. [32]

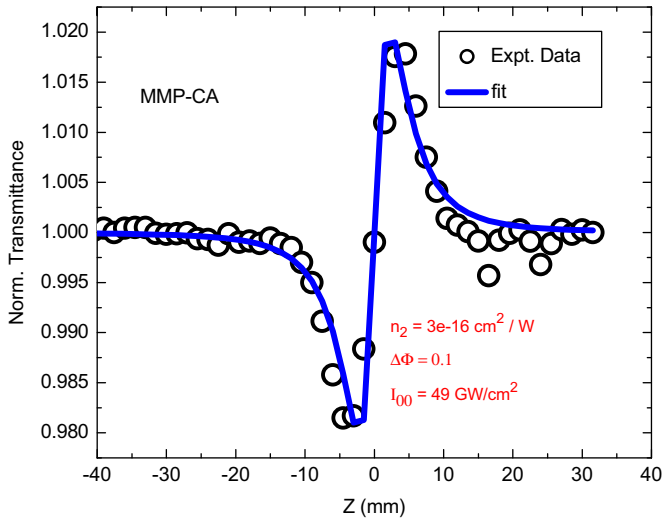

Fig. 10. Closed aperture Z-scan curve of the MMP sample. The solid line is a theoretical fit of the experimental data.

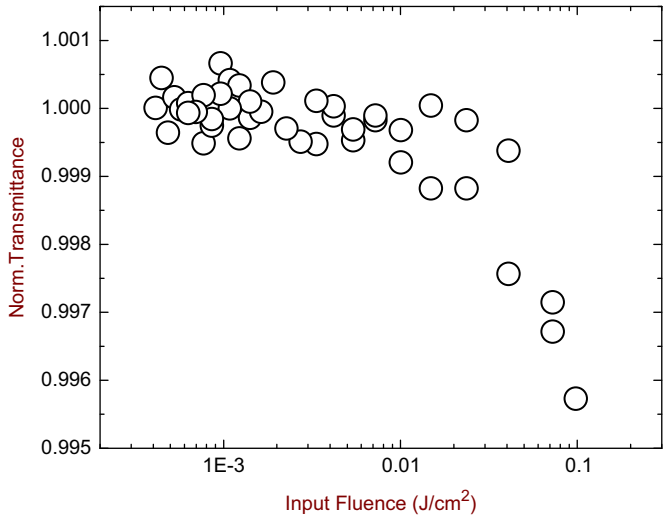

Fig. 11. Plot of normalized transmittance vs. input fluence.

have proposed asymmetric molecules for achieving large 2PA [6]. The present MMP crystal belongs to D–π–A system with elongated conjugation length which may be the reason for exhibiting third order NLO properties.

Optical limiting is a phenomena observed when the transmission of a medium decreases with increasing input laser intensity (or fluence). The present sample is transparent at the operating laser wavelength 800 nm. The relation for intensity dependent nonlinear absorption coefficient is given by [33]

$$dI/dz = -\beta I^2 \quad (2)$$

where β is the nonlinear absorption coefficient. The solution of Eq. (2) may be written as $I(z) = I_0/(1+\beta z I_0)$, where I_0 is the input intensity. Hence dynamic transmissivity can be given by $T(I_0,z) = I(z)/I_0 = 1/(1+\beta z I_0)$. Fig. 11 shows the optical limiting data obtained for the present sample. An effective optical limiter will have low limiting threshold, high optical damage threshold and stability, fast response time, high linear transmittance throughout the sensor band width, optical clarity and robustness. Materials that exhibit RSA usually show good optical limiting characteristics of the high intensity laser pulses. In order to observe RSA, the exited state absorption cross-section should be higher than that of the ground state absorption cross-section and is consistent with the present result. The excited state and ground state absorption cross-sections determined using the equation present in the literature [33] were found to be 5.09×10^{-19} cm^2 and 1.29×10^{-19} cm^2 respectively. Therefore, in this MMP crystal, the two-photon assisted excited state absorption leading to RSA may be responsible for the optical limiting action [34].

The utility of NLO crystal depends not only on the linear and NLO properties but also largely on its ability to withstand high power lasers [35]. Laser damage studies on NLO crystals are very important as the surface damage of the crystal by high-power lasers limits its performance in NLO applications. The crystal MMP has laser damage threshold of 4.26 GW/cm^2. The LDT value of MMP is comparable with high quality crystals like LAP, urea and BBO.

The refractive index value can be calculated using the equation $n = \tan\theta_p$, where θ_p is Brewster angle. Unlike inorganic materials, the organic crystals usually have transparency in the visible region. The values of refractive index 1.35 and 1.33 were obtained, respectively, for green and red laser light. We observed that there was not much variation in the value of refractive index in two different wavelengths of visible region indicating that there is no extra absorption in those corresponding wavelengths.

3.6. Dielectric properties

The different polarization mechanisms in solids such as atomic polarization of lattice, orientation polarization of dipoles, space charge polarization, electric and ionic polarizations can be understood easily by studying the variation of dielectric constant as a function of frequency and temperature. Fig. 12 represents the variation of dielectric constant with frequency. ε_r (dielectric constant) had high values in the lower frequency regions and then it decreased with the applied frequency. The high value at the low frequencies (100 Hz) may be due to the presence of all four polarizations and its low value at high frequencies may be due to the loss of significance of these polarizations gradually [36]. The response of dielectric constant with temperature is shown in Fig. 13. It was found that dielectric constant gradually increased with increase in temperature. This indicates the presence of space charge effect in addition to electronic and atomic conduction in the samples [37]. No abrupt changes are observed in the response indicating the absence of any phase transition; this was confirmed by the thermal studies.

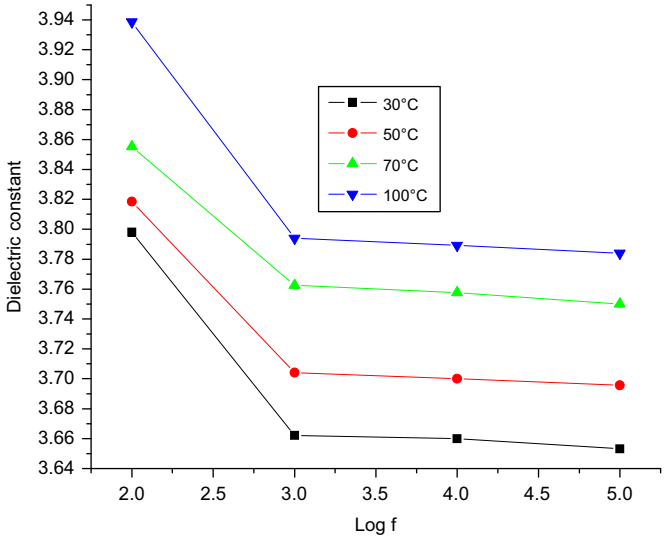

Fig. 12. Plot of dielectric constant vs. log f for MMP.

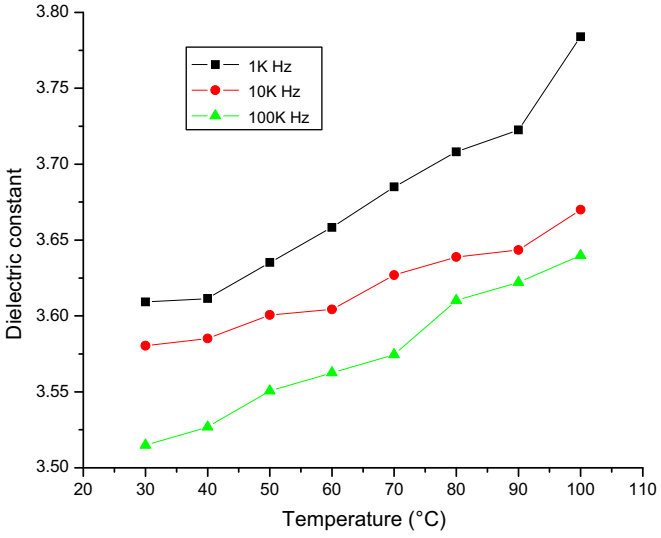

Fig. 13. Plot of dielectric constant vs. temperature for MMP.

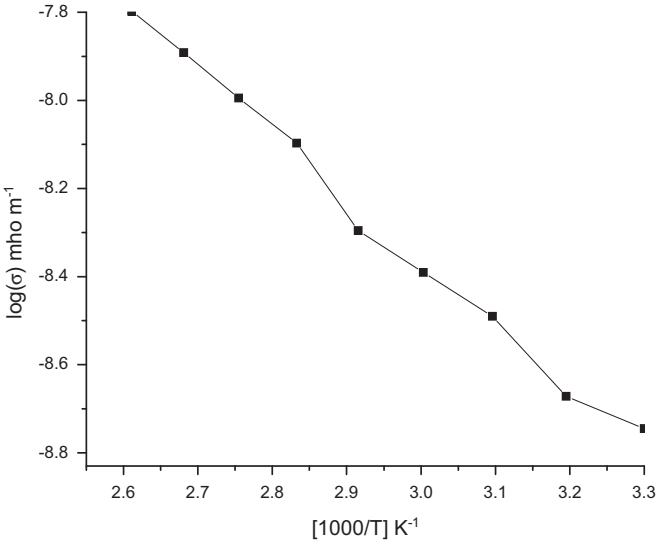

Fig. 15. Arrehenious plot.

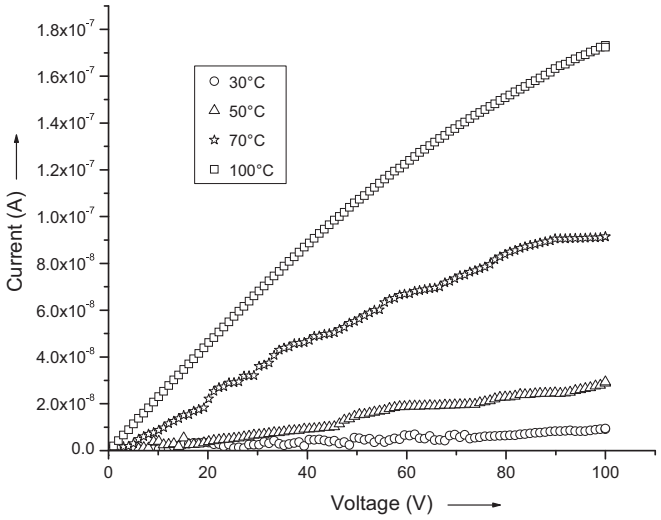

Fig. 14. Plot of current vs. voltage for MMP.

3.7. *Electrical properties*

The current voltage plots of crystal are shown in Fig. 14. The crystal MMP was electrically non-conducting at room temperature and its resistance estimated at 30 °C, from the slope of the linear graph, was found to be $1.2 \times 10^{10}\ \Omega$. The DC conductivity of the material was calculated using the relation [38] $\sigma = d/RA$, d=thickness of sample crystal, A=area of the face of the crystal in contact with electrode. The Arrhenius plot can be drawn by taking $\ln(\sigma)$ along x-axis and $(1000/T)$ along y-axis. The conductivity values can be fitted to the relation $\sigma = \sigma_0 \exp(-E/KT)$, where E is the activation energy, K is the Boltzmann constant, T represent absolute temperature and σ_0 is the parameter depending on the material. Activation energy can be estimated from the slope of above graph using the formula $E = -(\text{slope})\ K \times 1000$. The plot of $\ln(\sigma)$ vs. $(1000/T)$ for applied 50 V is given in the Fig. 15. The value of activation energy was found to be 0.124 eV. The crystal MMP has the activation energy value which is less than reported value of KDP (0.22 eV). The value of the activation energy provides the information that MMP crystal is semiconducting in nature.

4. Conclusions

A new nonlinear optical organic crystal 1-[4-({(*E*)-[4-(methylsulfanyl)phenyl]methylidene}amino)phenyl]ethanone was synthesized and single crystals of dimensions up to $4 \times 4 \times 2\ mm^3$ were grown by the slow evaporation technique in methanol. Single crystal X-ray diffraction study of the crystal revealed that the crystal belongs to noncentrosymmetric monoclinic system with space group $P2_1$. Various functional groups present in MMP were identified by FT-IR spectrum. MMP crystals are thermally stable up to 152.54 °C. Crystal have good transparency range beyond the cutoff (400 nm), extending into the IR region. The high energy gap values confirmed that at room temperature MMP crystals are insulators. This crystal has good SHG efficiency and its value is 4.13 times that of urea. This crystal exhibited third order nonlinear properties which are compared with reported chalcone crystals. The present sample exhibited good nonlinear optical coefficients obtained with ps laser pulses at 800 nm, which helps in designing the material for suitable device applications. The single shot laser damage threshold for MMP crystal was 4.26 GW/cm^2 and is comparable with high quality LAP, BBO, urea crystals. The influence of different polarizations mechanisms on the crystal was understood by the measurements of dielectric properties. MMP is an electrically nonconducting material at room temperature. Due to the presence of wide transparency range, good damage threshold value and high SHG efficiency, this crystal may be useful in NLO applications.

Acknowledgments

Authors acknowledge the Department of Science and Technology (DST), Government of India for financial assistance. We are grateful to SAIF Cochin and SAIF Madras for providing experimental facilities. The authors would like to thank, Mr. Deepak, School of Physics, University of Hyderabad, for his help in laser damage studies.

References

[1] Jordon G, Kobayashi T, Blau WJ, Pfeiffer S, Horhold H-H. Frequency upconversion of 800 nm ultrashort pulses by two-photon absorption in a stilbenoid compound-doped polymer optical fiber. Advanced Functional Materials 2003;13:751–4.

[2] Yang Z, Aravazhi S, Schneider A, Seiler P, Jazbisnek M, Gunter P. Synthesis and crystal growth of stilbazolium derivatives for second-order nonlinear optics. Advanced Functional Materials 2005;15:1072–6.
[3] Kwon O-P, Kwon S-J, Jazbisnek M, Brunner FDJ, Seo J-I, Hunziker C, et al. Organic phenolic configurationally locked polyene single crystals for electro-optic and terahertz wave applications. Advanced Functional Materials 2008;18:3242–50.
[4] Wong MS, Bosshard C, Gunter P. Crystal engineering of molecular NLO materials. Advanced Functional Materials 1997;9:837–42.
[5] Kiran AJ, Kim HC, Kim K, Rotermund F, Ravindra HJ, Dharmaprakash SM, et al. Superior characteristics of organic chalcone single crystals as efficient nonlinear optical material. Applied Physics Letters 2008;92:113307–10.
[6] John Kiran A, Lee HW, Ravindra HJ, Dharmaprakash SM, Kim K, Lim H, et al. Designing novel chalcone single crystals with ultra fast nonlinear optical responses and large multiphoton absorption coefficients. Current Applied Physics 2011;10:1290–6.
[7] Bosshard C, Sutter K, Prgtre P, Hulliger J, Florsheimer M, Kaatz P, et al. Organic nonlinear optical materials. Amsterdam: Gordon and Breach Science Publishers; 1995.
[8] Zyss J. Molecular nonlinear optics: materials, physics, devices. Boston: Academic Press; 1994.
[9] Prasad PN, Williams JD. Introduction to nonlinear optical effects in molecules and polymers. New York: Wiley; 1990.
[10] Chemla DS, Zyss J. Nonlinear optical properties of organic molecules and crystals. Orlando: Academic Press; 1987.
[11] Bosshard C, Sutter K, Schlesser R, Gunter P. Electro-optic effects in molecular crystals. Journal of the Optical Society of America B 1993;10:867–85.
[12] Zyss J. Hyperpolarizabilities of substituted conjugated molecules. III. Study of a family of donor–acceptor disubstituted phenyl-polyenes. Chemical Physics 1979;71:909–16.
[13] Levine BF, Bethea CG, Thurmond CD, Lynch RT, Berstein JL. An organic crystal with an exceptionally large optical secondharmonic coefficient: 2methyl4nitroaniline. Journal of Applied Physics 1979;50:2523–7.
[14] Prasad PN, Williams DJ. Introduction to nonlinear optical effects in organic molecules and polymers. New York: Wiley; 1991.
[15] Marder SR, Torruellas WE, Blanchard-Desce M, Ricci V, Stegeman GI, Gilmour S, et al. Large molecular third-order optical nonlinearities in polarized carotenoids. Science 1977;276:1233–6.
[16] Ravindra HJ, Chandrashekaran K, Harrison WTA, Dharmaprakash SM. Structure and NLO property relationship in a novel chalcone co-crystal. Applied Physics B 2009;94:503–11.
[17] Ravindra HJ, Harrison WTA, Suresh Kumar MR, Dharmaprakash SM. Synthesis, crystal growth, characterization and structure-NLO property relationship in 1,3-bis(4-methoxyphenyl)prop-2-en-1-one single crystal. Journal of Crystal Growth 2009;311:310–5.
[18] D'silva ED, Narayan Rao D, Philip Reji, Ray Butcher J, Rajnikant, Dharmaprakash SM. Synthesis, growth and characterization of novel second harmonic nonlinear chalcone crystal. Journal of Physics and Chemistry of Solids 2011;72:824–30.
[19] Sheldrick GM. SHELXS97 and SHELXL97. Germany: University of Göttingen; 1997.
[20] Kolev Ts, Koleva BB, Nikolova R, Seidel RW, Mayer-Figge H, Spiteller M, et al. 1,10-Phenanthrolinium hydrogensquarate monohydrate—a non-centrosymmetric structure from two non-chiral agents. Spectrochimica Acta Part A 2009;73:929–35.
[21] Haines PJ, editor. Thermal analysis principle; application and problems. London: Blackie Academic & Professional; 1987.
[22] Spek ALA. Multipurpose crystallographic tool. The Netherlands: University of Utretcht; 1998.
[23] D'silva ED, Narayan Rao D, Philip Reji, Ray Butcher J, Rajnikant, Dharmaprakash SM. Second harmonic chalcone crystal: synthesis, growth and characterization. Physica B: Condensed Matter 2011;406:2206–10.
[24] Tauc J, Grigorovici R, Vance A. Optical properties and electronic structure of amorphous germanium. Physica Status Solidi B 1966;15:627–37.
[25] Kurtz SK, Perry TT. A powder technique for the evaluation of nonlinear optical materials. Journal of Applied Physics 1968;39:3798–813.
[26] Sheik-Bahae M, Said AA, Van Stryland EW. High-sensitivity, single-beam n_2 measurements. Optics Letters 1989;14:955–7.
[27] Mathews SJ, Chaitanya Kumar S, Giribabu L, Venugopal Rao S. Nonlinear optical and optical limiting properties of phthalocyanines in solution and thin films of PMMA studied using a low power He–Ne laser. Materials Letters 2007;61:4426–31.
[28] Ravidra HJ, John Kiran A, Chandrasekharan K, Shashikala HD, Dharamprakash SM. Third order nonlinear optical properties and optical limiting in donor/acceptor substituted 4′-methoxy chalcone derivatives. Applied Physics B: Lasers and Optics 2007;88:105–10.
[29] Saito T, Yamaoka Y, Kimura Y, Morita R, Yamashita M. Femptosecond dynamics of nonresonant third-order optical nonlinearity of 1-(3-thienyl)-3-(4-chlorophenyl)propene-1-one crystal and solution. Japanese Journal of Applied Physics 1996;35:4649–53.
[30] Bosshard C, Spreiter R, Gunter P. Microscopic nonlinearities of two-component organic crystals. Journal of the Optical Society of America B 2011; 18:1620–6.
[31] Alabota M, Belijonne D, Bredas JL, Ehrlich JE, Fu JY, Heikal AA, et al. Design of organic molecules with large two-photon absorption cross sections. Science 1998;281:1653–6.
[32] Reinhardt BA, Brott LL, Clarson SJ, Dillard AG, Bhatt JC, Kannan R, et al. Highly active two-photon dyes: design, synthesis, and characterization toward application. Chemistry of Materials 1998;10:1863–74.
[33] Shettigar S, Umesh G, Chandrasekharan K, Sarojini BK, Narayana B. Studies on third order nonlinear optical properties of chalcone derivatives in polymer host. Optical Materials 2008;30:1297–303.
[34] Zhan Chuanlang, Xu Wei, Zhang Deqing, Li Dehuan, Lu Zhenzhong, Nie Yuxin, et al. Z-scan investigation of fifth-order optical nonlinearity induced by saturable-absorption from $(TBA)_2Ni(dmit)_2$: application for optical limiting. Journal of Materials Chemistry 2002;12:2945–8.
[35] Bhar GC, Chaudhary AK, Kumbhakar P. Study of laser induced damage threshold and effects of inclusions in some nonlinear crystals. Applied Surface Science 2000;161:155–62.
[36] Narasimha B, Choudhary RN, Rao KV. Dielectric properties of $LaPO_4$ ceramics. Journal of Materials Science 1988;23:1416–8.
[37] Akutagawa Tomoyuki, Takeda Sadamu, Hasegawa Tatsuo, Nakamura Takayoshi. Proton transfer and a dielectric phase transition in the molecular conductor (HDABCO+)2(TCNQ)3. Journal of American Chemical Society 2004;126:291–4.
[38] Anne Assencia A, Mahadevan CDC. Electrical conductivity measurements on ADP single crystals added with simple organic compounds. Bulletin of Material Science 2005;28:415–8.